

Structure of binary colloidal systems confined in a quasi-one-dimensional channel

Wen Yang,^{1,2} Kwinten Nelissen,³ Minghui Kong,^{4,*} Zhi Zeng,¹ and F. M. Peeters^{3,†}

¹Key Laboratory of Materials Physics, Institute of Solid State Physics, Chinese Academy of Sciences, P.O. Box 1129, Hefei 230031, China

²Graduate School of the Chinese Academy of Sciences, Beijing 100049, China

³Departement Fysica, Universiteit Antwerpen, Groenenborgerlaan 171, B-2020 Antwerpen, Belgium

⁴Institute of Plasma Physics, Chinese Academy of Sciences, Hefei, Anhui 230031, China

(Received 22 September 2008; published 23 April 2009)

The structural properties of a binary colloidal quasi-one-dimensional system confined in a narrow channel are investigated through modified Monte Carlo simulations. Two species of particles with different magnetic moment interact through a repulsive dipole-dipole force and are confined in a quasi-one-dimensional channel. The impact of three decisive parameters (the density of particles, the magnetic-moment ratio, and the fraction between the two species) on the transition from disordered phase to crystal-like phases and the transitions among the different mixed phases are summarized in a phase diagram.

DOI: [10.1103/PhysRevE.79.041406](https://doi.org/10.1103/PhysRevE.79.041406)

PACS number(s): 82.70.Dd, 36.40.Sx, 52.27.Lw

I. INTRODUCTION

Self-assembly of confined low dimensional field-responsive systems has risen strong interest in recent years. Part of the interest arises from the fact that it is an ideal model to understand a variety of phenomena in condensed-matter physics. Moreover, it has huge practical applications in the fabrication of many new materials, such as special nanoscale magnetic dot arrays [1,2] which are the potential materials for high-density magnetic data storage, field response fabrics [3], and DNA separation devices [4]. Accordingly, numerous experimental and theoretical studies investigated a wide variety of such systems, e.g., two-dimensional (2D) Wigner-type crystals [5] or quasi-one-dimensional (Q1D) chains [6,7] formed in dusty plasmas, colloidal systems restricted in a circular hard wall [8,9] or in a Q1D channel [10–14], and superparamagnetic colloidal particles or hard disks at the liquid-air interface [15,16]. Among all these above systems, suspensions of superparamagnetic colloids trapped in the water-air interface has inspired unique interests because of its accessibility by experiments [17–19] which has resulted in extensive studies using computer simulations [15,20,21]. Similar paramagnetic colloids on surfaces were investigated as well [22,23].

Furthermore, most of these existing studies of 2D systems were focused on the ground-state structure [5,8,15,20], thermodynamics including normal modes [5], melting behavior [5,8], and dynamic processes [17]. While for Q1D systems a lot of attention was paid on the edge effect of the confining channel [10], the dependence of the structure upon the width of the external channel [14,24], re-entrant solid-liquid phase transition [11,25], heat transport behavior [12,26], transition from 2D to three-dimensional (3D) [27], closest packing property [28], and so on were also investigated.

Here we consider superparamagnetic colloids that are confined in a Q1D channel as, e.g., studied in [13,14]. In

contrast to previous work [14] where a monodisperse system was investigated, we extend this previous work to a binary system. Very recently, the scientific focus of both theoretical and experimental studies of confined systems shifted to the study of two-species systems, e.g., systems with two types of charged particles, which was motivated by the increased complexity of the phase diagrams [29]. The structure and melting of heterogeneous systems made of single and double charged species with the same mass were studied in Ref. [30]. Nelissen *et al.* [31] studied the ground state of a finite-size system containing one or two impurities with different charge and mass, which was motivated by the experiment of Ref. [32]. Static and dynamical properties of a binary system trapped in a dusty plasma or circular hard wall were studied both theoretically [33–36] and experimentally in Refs. [37–39]. Liu *et al.* [40] even extended the analysis from binary to multispecies systems. Concerning the superparamagnetic colloidal binary systems, different types of stable crystallites have been found [18–21] and also glassy dynamics could occur [15,17].

All of the above studies considered binary systems in a 2D confinement. Very recently a Q1D system of particles interacting through a repulsive Yukawa potential and confined in a parabolic trap [41] was studied theoretically, and a rich phase diagram of different ordered structures was obtained. Both continuous and discontinuous structural transitions were found and even a disordered phase which was the ground state in a small region of the parameter space. Here, we consider a similar system but with dipole interparticle interaction and hard wall confinement. Our system models an experimental realizable system of paramagnetic colloids moving through a lithographic defined channel. The main differences with the system studied in Ref. [41] are (i) the long-range interparticle interaction and (ii) the nonuniform particle density. Such study has never been done before. Our study is motivated by the recent experiments of 3D binary colloidal systems [42,43], and the simulations of the phase diagram of 3D and 2D binary colloidal systems in Refs. [44,45]. In this paper we will discuss the dependence of the ground-state configuration of binary systems on the magnetic moment and the fraction of the two species.

*mhkong@cashq.ac.cn

†francois.peeters@ua.ac.be

The paper is organized as follows. In Sec. II, the model and the numerical approach are described. Typical ground-state configurations and phase diagram for binary systems with different magnetic-moment ratio between the two species and different fraction of the two kinds of particles are discussed in Sec. III. Our conclusions are given in Sec. IV.

II. NUMERICAL APPROACH

We study the properties of a binary system confined in a Q1D channel, namely, a binary colloidal system confined by two parallel hard walls (Q1D channel). Such colloids have macroscopic magnetic moment in the presence of an external magnetic field [14,39], which is directed perpendicular to the 2D plane where the particles are moving in. The interaction between the colloids is given by a repulsive magnetic dipole potential. Our system consists of two different kinds of particles, i.e., the small particles N_s with magnetic moment M_s and the big particles N_b with a larger magnetic moment M_b . The magnetic-moment ratio between these two kinds of particles is defined as $M_r = M_s/M_b < 1$, with the value of M_b fixed and M_s varied. The induced magnetic moment is chosen to be proportional to the mass and volume of the particles. The energy of such a Q1D system is given by

$$H = \sum_{i=1}^N V(R_i) + \frac{\mu_0 M_s^2}{4\pi R_w^3} \sum_{i>j=1}^{N_s} \frac{R_w^3}{|\vec{R}_i - \vec{R}_j|^3} + \frac{\mu_0 M_b^2}{4\pi R_w^3} \sum_{k>l=1}^{N_b} \frac{R_w^3}{|\vec{R}_k - \vec{R}_l|^3} + \frac{\mu_0 M_s M_b}{4\pi R_w^3} \sum_{m=1}^{N_s} \sum_{n=1}^{N_b} \frac{R_w^3}{|\vec{R}_m - \vec{R}_n|^3}, \quad (1)$$

with the channel confining potential taken as

$$V(R) = \begin{cases} 0 & \text{for } |y| \leq R_w/2 \\ \infty & \text{for } |y| > R_w/2. \end{cases} \quad (2)$$

In the above formulas N represents the total number of particles ($N = N_s + N_b$), μ_0 represents the magnetic permeability of free space, R_w represents the width of the channel trap (distance between the two parallel hard walls), and $\vec{R}_i = (x_i, y_i)$ represents the position of the i th particle with $|y_i| \leq R_w/2$. The colloidal particles move typically in a nonmagnetic liquid which makes their motion overdamped.

We rewrite the energy in a dimensionless form and choose R_w as unit of length, $E_0 = \mu_0 M_b^2 / 4\pi R_w^3$ as unit of energy, and M_b as unit of magnetic moment. Equation (1) then reads as follows:

$$H = \sum_{i>j=1}^{N_s} \frac{M_r^2}{|\vec{r}_i - \vec{r}_j|^3} + \sum_{k>l=1}^{N_b} \frac{1}{|\vec{r}_k - \vec{r}_l|^3} + \sum_{m=1}^{N_s} \sum_{n=1}^{N_b} \frac{M_r}{|\vec{r}_m - \vec{r}_n|^3}, \quad (3)$$

with the hard wall potential in the form

$$V(r) = \begin{cases} 0 & \text{for } |y| \leq 0.5 \\ \infty & \text{for } |y| > 0.5. \end{cases} \quad (4)$$

According to Eq. (3), the structure of the system only depends on the total number of particles, i.e., its density (ρ),

the magnetic-moment ratio (M_r), and the fraction (N_s, N_b) of the two kinds of particles.

To simulate such Q1D systems, a unit box containing N particles with fixed width ($\equiv 1$) and fixed length ($\equiv 15$) was used with periodic boundary conditions (PBC) imposed in the x direction and hard wall boundaries in the y direction. We increased the length of the simulation box with a factor of 10 in order to check that the results are qualitatively the same and quantitatively within our numerical error bars. Thus the density of the total number of particles is given by $\rho = N/(15R_w)$, and increasing N is equivalent to the increase in the density. The ground-state energy and configurations of a N -particle unit box was obtained. In order to ensure the obtained energy was very close to the global minimum, annealing simulations were used to cool down the system from a nonzero temperature T_0 to zero temperature through

$$T_s(i) = T_0 \left(\frac{T_E}{T_0} \right)^{i/N_i} - T_E, \quad (5)$$

$$T_b(i) = \frac{T_s(i)}{2}, \quad (6)$$

where N_i is the total number of annealing steps, T_E is a temperature close to zero, and $T_s(i)$ and $T_b(i)$ are the temperatures of the small particles and the big particles, respectively, for the i th annealing cycle. As shown in Eq. (6), $T_b(i)$ is half of $T_s(i)$ because we make the reasonable assumption that the big particles can be stabilized faster than the small particles. Different annealing schedules were tested and compared before obtaining the most efficient one which is given by Eqs. (5) and (6).

III. RESULTS

Most of the previous studies were focused on the dependence of the ordered Q1D structure on the width of the confining channel [14,24]. One of the essential findings is that, when the width of the channel is increased, under identical number density ($\rho = N/A$, where A is the area of the simulation box), an increasing number of layers is observed.

To prove the validity of our model system and methodology we show in Fig. 1, the ground-state configurations of monodisperse systems with density ρ varied from 5.33 to 10.67. Seen from top to bottom of Fig. 1, the density of the particles is increased, which drive the particles to separate into more layers. At first glance, the configurations in Fig. 1 are close to a hexagonal latticelike structure. However, after further inspection, we found that some of the structures actually have more lattice defects than the others, such as in the case for $\rho = 6.67, 8$. For $\rho = 8$, the formed structure is a transition structure from the three-layer to the four-layer hexagonal latticelike configuration. A similar transition occurs from the two-layer structure to the three-layer structure around $\rho = 6.67$. This indicates that all the defect-rich lattices are virtually transitional structures before a hexagonal lattice with more layers is formed with increasing density. In order to understand this transition better, we plotted the ratio of the number of defects in the center of the system to the total

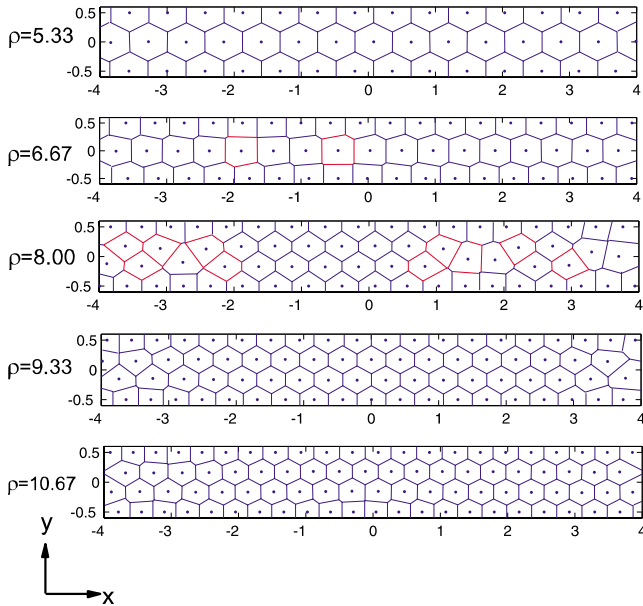


FIG. 1. (Color online) Snapshots of the ground-state configurations (only part of the unit cell is shown) of monodispersed systems with densities $\rho=5.33, 6.67, 8.9.33,$ and 10.67 which is marked on the left side of the figure. The defects in the middle of the channel are marked by red polygons.

number of the inner particles in Fig. 2. A defect here is defined as a particle with more or less six nearest neighbors, excluding the particles at the edge. This plot shows clearly that if one increases the density, the relative number of defects in the system is oscillating. The oscillations are explained by the fact that the system tries to form a Wigner lattice structure. A nearly perfect Wigner structure can only be formed at certain particle densities. The configurations corresponding with the local minima in Fig. 2 are analogous to the configurations with magic-number channel widths in the similar system of Ref. [14]. The consistency of these results clearly confirms the validity of our model system and methodology. This study on monodisperse systems will be a

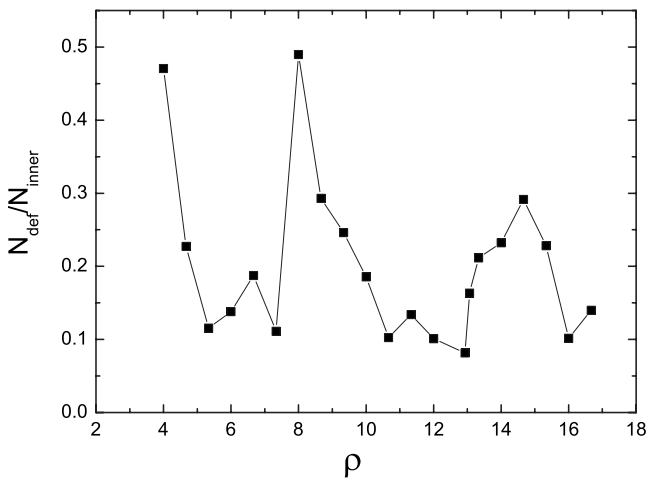


FIG. 2. Ratio of defect particles to the total number of inner channel particles in a monodisperse Q1D system as function of the density of particles.

guide to our study of the more complicated binary systems.

In what follows, we systematically study the properties of the ground-state configuration of binary systems. From Eq. (3) we know that the properties of the system are mostly determined by the magnetic-moment ratio (M_r), the fraction of the small particles $F_s=N_s/N$, and the particle density (ρ).

For 2D binary systems [30,35] and Q1D binary systems [41] studied before, the ground state consisted of ordered crystal structures. However, we found that for our Q1D binary system with hard wall confinement, the ground state has a plethora of phases including disordered and crystal-like phases.

In Fig. 3, the configuration of a binary system with $\rho=9.33$ is shown for $M_r=0.1-0.5$ and $F_s=0.1, 0.3, 0.6,$ and 0.8 . If F_s and M_r are small [Fig. 3(a)], all the small particles (black full dots) are located as interstitials between the big particles (red open circles). Here the magnetic-moment asymmetry is strong, i.e., the magnetic moment of small particles is much smaller than that of the big particles. Thus the dipole-dipole interaction (coupling) between the small particles and big particles is much smaller than those between the big particles. As a result, the small particles can be locally trapped by the big particles which is illustrated by the small cage in Fig. 3(a). This phase will be called the “particle-interstitial” phase. In this phase most of the small particles will be surrounded by five big particles. Such a particle-interstitial structure will have very different diffusion properties which will be discussed in our following work.

For larger M_r (i.e., the coupling between the particles becomes stronger), as shown in Fig. 3(c), the small particles tend to form a similar crystal structure, as found for a monodisperse system (see Fig. 1), together with the big particles. When the magnetic-moment asymmetry is small as in Fig. 3(c), the interaction between the small and big particles becomes comparable to the interaction between the big particles. Because the two species become almost indistinguishable, this state will be further referred to the substitutional phase. Here in this phase most of the small particles will be surrounded by six big particles. This explains why the binary systems of Figs. 3(c) have similar structures as the corresponding monodisperse systems with the same density.

If one now increases F_s to 0.30 at $M_r=0.1$ as shown in Fig. 3(d), multiple small particles will form clusters of small particles as interstitials between the big particles. These big particles will behave as local cages for the small particles grouped in clusters. These clusters of small particles can be seen as one effective particle by the surrounding particles. Therefore we will call this phase the “cluster-interstitial” phase which can also be seen as an extension of the particle-interstitial phase. This structure is a disordered phase rather than a crystal-like phase.

If one increases $M_r=0.1$ to $M_r=0.5$ [Fig. 3(f)] further, one finds again the substitutional phase but with the difference that now the particles can be located at the edge of the system in contrast to Fig. 3(c).

If one increases F_s further to 0.6 at $M_r=0.1$, due to the increasing number of small particles, the previously separated “interstitial clusters” become linked and form a chain-like structure of small particles, which we will call the

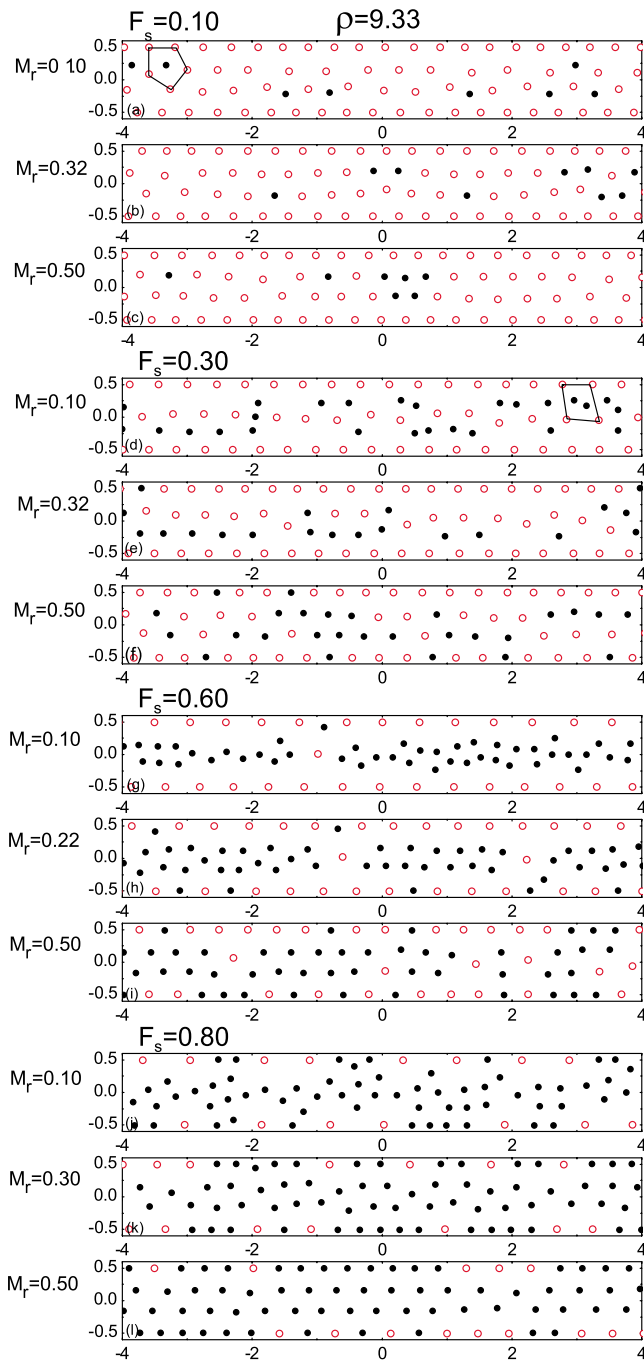


FIG. 3. (Color online) Typical ground-state configurations of binary systems (only part of the unit cell) for $\rho=9.33$. The corresponding parameters (ρ, F_s, M_r) of each configuration are marked. The open circles (red) denote the particles with big magnetic moment, while the full dots (black) refer to the particles with small magnetic moment.

“chain” structure. For such chain structure, the density of particles inside the channel can be higher than that at the edge, a situation which does not occur in single-species systems [14]. The emergence of this chain structure breaks the general rule obtained from the monodisperse system that there are always more particles at the edge than at the inside of the confining channel. Similar as the cluster-interstitial structure, this structure is a disordered structure.

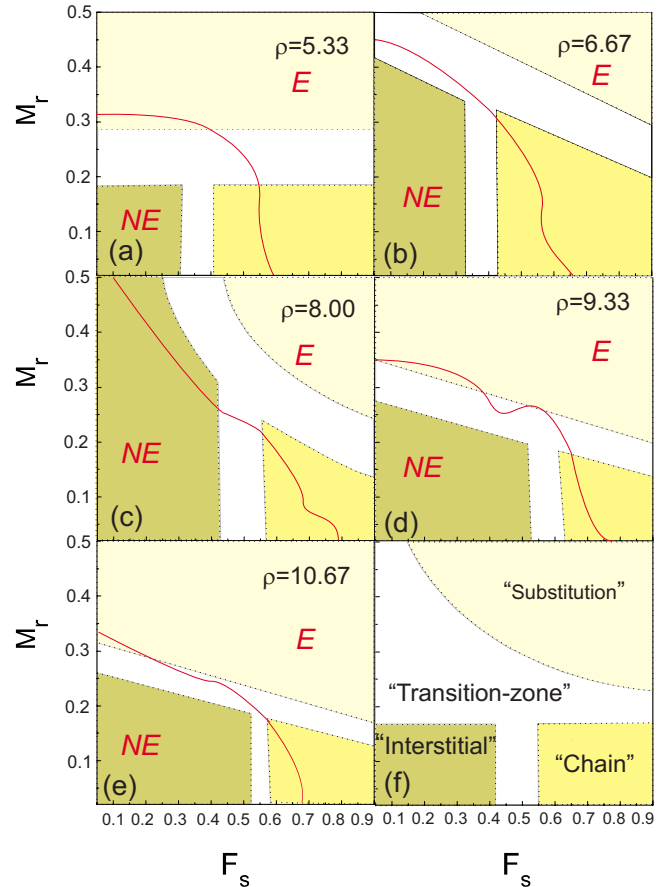


FIG. 4. (Color online) Phase diagram of binary systems confined into a hard wall channel for six different densities from $\rho = 5.33$ up to 10.67. The white transition zone separates three phases: the interstitial, the substitutional, and the chain phases. The red line separate two subphases: one where big and small particles are mixed at the edge (indicated by *E*) and another where there is no mixing (indicated by *NE*).

If one increases M_r to 0.5 as in Fig. 3(i), again a crystal-line substitutional structure is formed. Finally if one increases F_s to 0.8 at $M_r=0.1$, one will find a “chainlike” structure of small particles in the center with some of the small particles at the edge of the channel.

So far we looked at the effect of changing F_s at constant magnetic dipole ratio M_r . Now we will investigate how a system is going from a disordered state to a crystal structure by changing the magnetic-moment ratio at constant F_s . If one decreases the magnetic-moment ratio M_r of the system from $M_r=0.1$ to $M_r=0.5$ in Figs. 3(j)–3(l), one will go gradually from the disordered chain structure to the crystal-like substitutional structure while keeping the ρ and F_s unchanged.

We summarized our findings in Fig. 4(d), into a phase diagram of the magnetic ratio M_r (0.02–0.50) versus the fraction of small particles F_s (0.05–0.90) for $\rho=9.33$. For the construction of the phase diagram, the step size when varying M_r is taken to be 0.02 and when varying F_s is chosen to be 0.05. In this phase diagram we concentrate on three phases: the “interstitial” phase (taken the “cluster” and particle-interstitial phase together), the chain, and the “substitutional” phase. Because the transition from one to another

phase occurs gradually, the transition region from one phase to another is indicated by a white transition zone which has a T-like shape. This T-like shape can be explained as follows. If one increases the fraction of small particles from 0 to 0.9 at $M_r=0.1$ one will go through a phase transition from the interstitial phase to the chainlike phase as expected. If one increases M_r from 0 to higher values one will go from the interstitial or chain phase to the substitutional phase because small particles become indistinguishable from the other particles. If one increases F_s at $M_r=0.1$, the small particles will first fill the holes between the bigger particles as interstitials. If one increases F_s further, these interstitial particles will agglomerate as interstitial clusters between the big particles and finally repel most of the big particles out of the center forming a chainlike structure. (Please note that these chains are different from the chains formed when the dipoles are aligned along the chain. Here the dipole moments are still directed perpendicular to the chain.) If one however increases F_s from 0 to 0.9 at $M_r=0.4$ the system will undergo a phase transition from the interstitial phase to the substitutional phase. Figure 1 shows that a perfect Wigner structure can only be formed at certain particle densities. If there are a lot of lattice defects in the system (corresponding with local maxima in the curve) those vacancies will be filled with small particles as interstitials between the big particles. If the fraction of small particles becomes large enough to fix the disordered triangular Wigner lattice, those small particles become substitutional. At the other hand if the big particles already form a quasiperfect (close packed) Wigner crystal, for systems corresponding with the local minima in Fig. 2, the small particles will be rather inserted as substitutional in order to conserve the Wigner structure. This effect is clearly visible if one compares the different phase diagrams. For $\rho=5.33$ and $\rho=10.67$, the phase boundary between the interstitial and the substitutional phases is quasihorizontal because the big particles are forming a quasiperfect Wigner crystal. For $\rho=6.67$, 8, and 9.33 the big particles form a pattern with a lot of lattice defects. If the small particles are inserted in a structure similar to this, they will never form a regular structure because of the chaotic organization of the big particles in the center of the system. This makes that the inclination of this phase boundary is proportional with the number of defects in the system. Further we can see from this phase diagram that the phase boundary between the interstitial phases is shifted to the right as function of the density. The reason is that the particles in a monodisperse system with a higher density of particles are strongly coupled. This makes it very difficult for the particles to break the crystalline structure of the small particles resulting in a shift of the phase boundary. Further we distinguish whether the small and big particles are mixed or not at the edge of the system (we define the mixing state where more than 10% of small particles stay at the edge) indicated by the red line in the phase diagram.

For the interstitial and substitutional phases the mixing of the big and small particles at the edge of the system is easy to understand. In the substitutional phase, there is a very small difference between the small and big particles; consequently they can substitute each other both in the center as well as at the edge of the channel. This phase is therefore

characterized by the mixing of the particles at the edge of the confinement. In the interstitial phase, however, the small particles are trapped between the big particles and consequently are not located at the edge of the confinement. In the chain phase, however, particles can be located at the edge if the density of small particles is large enough. This is because at high concentration of small particles, the big particles are not able to trap the small particles as interstitials. The mixing and nonmixing phases are separated in the phase diagram by the red line. From this we can conclude that there are two mechanisms responsible for mixing of particles at the edge: (i) the fraction of the small particles becomes so large that some of them are forced to occupy an edge position and (ii) the small particles become indistinguishable from the big particles because of the too small difference in magnetic moment.

IV. CONCLUSION

The problem of whether the two species in a binary system are separated or mixed has always been a very important topic in the research of binary systems. Previous works found a general rule valid for 2D binary systems confined in a circular external potential: independently of confining the particles in a parabolic trap [30] or a hard wall [35], the big particles always stay at the edge of the trap, while the small particles appeared inside. Even this rule was found to apply for Q1D systems trapped in a parabolic potential [41]. Here we studied the structural properties of classical quasi-one-dimensional binary systems confined in a narrow channel which was investigated through modified Monte Carlo simulations, and this rule was found to be no longer valid.

The impact of three decisive parameters (the density of particles ρ , the fraction of small particles F_s , and magnetic-moment ratio M_r) on the structure were discussed in detail. Depending on these three parameters the particles in the system will be organized in the interstitial, chain, or substitutional," structure. If the fraction of small particles F_s is small, each small particle is surrounded by five nearest neighbors, and one can speak about a particle-interstitial. If one increases F_s , more small particles will be grouped in clusters forming the cluster-interstitial structure. If F_s becomes very large, a chainlike structure of small particles will be formed in the center. At the other hand the phase is determined by the density which determines the number of layers in the system as found for a monodisperse system.

Besides the structural transitions, we also investigated the mixing state of the two species of particles distinguishing two phases: mixing of big and small particles at the edge of the channel or not. If the magnetic-moment asymmetry is weak, we can distinguish two phases a phase where one can find substitutionals at the edge and one where there are no substitutionals. This means that if the small particles are inserted in the system as substitutional, they prefer to be substituted in the center. If F_s becomes larger the probability of finding small particles at the edge is increased. When the magnetic asymmetry is larger, the probability of finding a small particle at the edge is reduced and the two particles are not mixed. From this we can conclude that the small particles

prefer to stay at the center while the big particles tend to be at the edge.

ACKNOWLEDGMENTS

This work was supported by the China-Flanders bilateral project, the National Science Foundation of China under Grants No. 10774148 and No. 10504036, the special funds for Major State Basic Research Project of China (973) under

Grant No. 2007CB925004, Knowledge Innovation Program of Chinese Academy of Sciences, and Director Grants of CASHIPS. This work was partly supported by the SRF for ROCS, SEM. Part of the calculations were performed in the Center for Computational Science of CASHIPS, the Shanghai Supercomputer Center, and CalcUA (University of Antwerp). We acknowledge discussions with V. R. Misko and B. Partoens and support from the Flemish Science Foundation (FWO-VI).

-
- [1] J. Y. Cheng, C. A. Ross, V. Z. H. Chan, E. L. Thomas, R. G. H. Lammertink, and G. J. Vancso, *Adv. Mater. (Weinheim, Ger.)* **13**, 1174 (2001).
- [2] H. C. Kim, X. Q. Jia, C. M. Stafford, D. H. Kim, T. J. McCarthy, M. Tuominen, C. J. Hawker, and T. P. Russell, *Adv. Mater. (Weinheim, Ger.)* **13**, 795 (2001).
- [3] Y. S. Lee, E. Wetzel, and N. Wagner, *J. Mater. Sci.* **38**, 2825 (2003).
- [4] P. S. Doyle, J. Bibette, A. Bancaud, and J.-L. Viovy, *Science* **295**, 2237 (2002).
- [5] V. M. Bedanov and F. M. Peeters, *Phys. Rev. B* **49**, 2667 (1994).
- [6] B. Liu, K. Avinash, and J. Goree, *Phys. Rev. Lett.* **91**, 255003 (2003).
- [7] G. Piacente, F. M. Peeters, and J. J. Betouras, *Phys. Rev. E* **70**, 036406 (2004).
- [8] R. Bubeck, C. Bechinger, S. Nesper, and P. Leiderer, *Phys. Rev. Lett.* **82**, 3364 (1999).
- [9] M. Kong, B. Partoens, A. Matulis, and F. M. Peeters, *Phys. Rev. E* **69**, 036412 (2004).
- [10] R. A. Segalman, A. Hexemer, and E. J. Kramer, *Phys. Rev. Lett.* **91**, 196101 (2003).
- [11] R. Haghgooeie, C. Li, and P. S. Doyle, *Langmuir* **22**, 3601 (2006).
- [12] A. Chaudhuri, S. Sengupta, and M. Rao, *Phys. Rev. Lett.* **95**, 266103 (2005).
- [13] M. Köppl, P. Henseler, A. Erbe, P. Nielaba, and P. Leiderer, *Phys. Rev. Lett.* **97**, 208302 (2006).
- [14] R. Haghgooeie and P. S. Doyle, *Phys. Rev. E* **70**, 061408 (2004).
- [15] N. Hoffmann, F. Ebert, C. N. Likos, H. Löwen, and G. Maret, *Phys. Rev. Lett.* **97**, 078301 (2006).
- [16] L. R. E. Cabral, B. J. Baelus, and F. M. Peeters, *Phys. Rev. B* **70**, 144523 (2004).
- [17] H. König, R. Hund, K. Zahn, and G. Maret, *Eur. Phys. J. E* **18**, 287 (2005).
- [18] F. Ebert, P. Keim, and G. Maret, *Eur. Phys. J. E* **26**, 161 (2008).
- [19] N. Osterman and D. Babič, I. Poberaj, J. Dobnikar, and P. Zihnerl, *Phys. Rev. Lett.* **99**, 248301 (2007).
- [20] J. Fornleitner, F. L. Verso, G. Kahl, and C. N. Likos, *Soft Matter* **4**, 480 (2008).
- [21] N. Hoffmann, C. N. Likos, and H. Löwen, *J. Phys.: Condens. Matter* **18**, 10193 (2006).
- [22] K. J. Mutch, V. Koutsos, and P. J. Camp, *Langmuir* **22**, 5611 (2006).
- [23] P. D. Duncan and P. J. Camp, *Phys. Rev. Lett.* **97**, 107202 (2006).
- [24] A. Ricci, P. Nielaba, S. Sengupta, and K. Binder, *Phys. Rev. E* **74**, 010404(R) (2006).
- [25] A. Ghazali and J.-C. S. Levy, *Europhys. Lett.* **74**, 355 (2006).
- [26] D. Chaudhuri, A. Chaudhuri, and S. Sengupta, *J. Phys.: Condens. Matter* **19**, 152201 (2007).
- [27] R. Haghgooeie and P. S. Doyle, *Phys. Rev. E* **75**, 061406 (2007).
- [28] S. Nesper, C. Bechinger, P. Leiderer, and T. Palberg, *Phys. Rev. Lett.* **79**, 2348 (1997).
- [29] M. E. Leunissen, C. G. Christova, A.-P. Hynninen, C. P. Royall, A. I. Campbell, A. Imhof, M. Dijkstra, R. van Roij, and A. van Blaaderen, *Nature (London)* **437**, 235 (2005).
- [30] J. A. Drocco, C. J. Olson Reichhardt, C. Reichhardt, and B. Jankó, *Phys. Rev. E* **68**, 060401(R) (2003).
- [31] K. Nelissen, B. Partoens, and F. M. Peeters, *Phys. Rev. E* **69**, 046605 (2004).
- [32] B. A. Grzybowski, X. Jiang, H. A. Stone, and G. M. Whitesides, *Phys. Rev. E* **64**, 011603 (2001).
- [33] W. P. Ferreira, F. F. Munarin, K. Nelissen, R. N. Costa Filho, F. M. Peeters, and G. A. Farias, *Phys. Rev. E* **72**, 021406 (2005).
- [34] W. P. Ferreira, F. F. Munarin, G. A. Farias, and F. M. Peeters, *J. Phys.: Condens. Matter* **18**, 9385 (2006).
- [35] W. Yang, M. H. Kong, M. V. Milosevic, Z. Zeng, and F. M. Peeters, *Phys. Rev. E* **76**, 041404 (2007).
- [36] K. Nelissen, B. Partoens, I. Schweigert, and F. M. Peeters, *Europhys. Lett.* **74**, 1046 (2006).
- [37] B. A. Grzybowski, H. A. Stone, and G. M. Whitesides, *Nature (London)* **405**, 1033 (2000).
- [38] L. Hornekær, N. Kjærgaard, A. M. Thomsen, and M. Drewsen, *Phys. Rev. Lett.* **86**, 1994 (2001).
- [39] K. Mangold, J. Birk, P. Leiderer, and C. Bechinger, *Phys. Chem. Chem. Phys.* **6**, 1623 (2004).
- [40] Y. H. Liu, Z. Y. Chen, M. Y. Yu, L. Wang, and A. Bogaerts, *Phys. Rev. E* **73**, 047402 (2006).
- [41] W. P. Ferreira, J. C. N. Carvalho, P. W. S. Oliveira, G. A. Farias, and F. M. Peeters, *Phys. Rev. B* **77**, 014112 (2008).
- [42] A. Yethiraj and A. V. Blaaderen, *Nature (London)* **421**, 513 (2003).
- [43] J. Baumgartl, R. P. A. Dullens, M. Dijkstra, R. Roth, and C. Bechinger, *Phys. Rev. Lett.* **98**, 198303 (2007).
- [44] A.-P. Hynninen and M. Dijkstra, *Phys. Rev. Lett.* **94**, 138303 (2005).
- [45] L. Assoud, R. Messina, and H. Lowen, *EPL* **80**, 48001 (2007).